Heparanase Gene Silencing, Tumor Invasiveness, Angiogenesis, and Metastasis

Evgeny Edovitsky, Michael Elkin, Eyal Zcharia, Tamar Peretz, Israel Vlodavsky

Background: **Heparanase is an endoglycosidase that degrades heparan sulfate, the main polysaccharide constituent of the extracellular matrix and basement membrane. Expression of the heparanase gene is associated with the invasive, angiogenic, and metastatic potential of diverse malignant tumors and cell lines. We used gene-silencing strategies to evaluate the role of heparanase in malignancy and to explore the therapeutic potential of its specific targeting.** ***Methods:*** **We designed plasmid vectors to express hammerhead ribozymes or small interfering RNAs (siRNAs) directed against the human or mouse heparanase mRNAs. Human breast carcinoma (MDA-MB-435) and mouse lymphoma (Eb) and melanoma (B16-BL6) tumor cell lines, which have naturally high levels of endogenous heparanase or have been genetically engineered to overexpress heparanase, were transfected with anti-heparanase ribozyme or siRNA. Semiquantitative reverse transcription–polymerase chain reaction (RT-PCR) and measurements of enzymatic activity were used to confirm the efficient silencing of heparanase gene expression. Cells transfected with the anti-heparanase ribozyme and siRNA vectors were tested for invasiveness *in vitro* and metastatic dissemination in animal models of experimental and spontaneous metastasis.** ***Results:*** **Compared with cells transfected with control constructs, cells transfected with the anti-heparanase ribozyme or siRNA vectors had profoundly reduced invasion and adhesion *in vitro,* regardless of cell type, and expressed less heparanase.** ***In vivo,*** **tumors produced by cells transfected with the anti-heparanase ribozyme and siRNA vectors were less vascularized and less metastatic than tumors produced by cells transfected with the control vectors. Mice injected with cells transfected with the anti-heparanase ribozyme and siRNA vectors lived longer than mice injected with control cells.** ***Conclusions:*** **The association of reduced levels of heparanase and altered tumorigenic properties in cells with anti-heparanase ribozyme- or siRNA-mediated gene-silencing vectors suggests that heparanase is important in cancer progression. Heparanase gene silencing has potential use as a target for anticancer drug development. [J Natl Cancer Inst 2004;96:1219–30]**

Tumor development, neovascularization, and metastatic spread depend on the ability of cancer cells to invade tissue barriers in a process involving degradation of the extracellular matrix (ECM) and basement membrane structures *(1–3).* Basement membranes underlie epithelial and endothelial cell layers and form a structural network of characteristic proteins and polysaccharides *(3,4).* Heparan sulfate glycosaminoglycan, the principal polysaccharide component of the basement membrane, is composed of repeating disaccharide units that form linear chains covalently bound to a core protein *(4,5).* Heparan sulfate chains interact through specific attachment sites with the main protein components of basement membrane and ECM, such as collagen IV, laminin, and fibronectin. Heparan sulfate is therefore a key element in the self-assembly, insolubility, and barrier properties of basement membrane and other types of ECM *(2–5).*

Affiliations of authors: Department of Oncology, Hadassah-Hebrew University Medical Center, Jerusalem, Israel (EE, ME, EZ, TP); Cancer and Vascular Biology Research Center, Bruce Rappaport Faculty of Medicine, Technion, Haifa, Israel (IV).

Correspondence to: Israel Vlodavsky, PhD, Cancer and Vascular Biology Research Center, Bruce Rappaport Faculty of Medicine, Technion, Haifa, 31096, Israel (e-mail: vlodavsk@cc.huji.ac.il).

See "Notes" following "References."

DOI: 10.1093/jnci/djh230

Journal of the National Cancer Institute, Vol. 96, No. 16,

In addition, heparan sulfate moieties in the ECM are responsible for specific binding of members of the heparin-binding family of growth factors (i.e., bFGF, VEGF, KGF, HGF) and serve as the extracellular reservoir for these factors *(4–6).* Thus, within the ECM, heparan sulfate–bound growth and angiogenic factors are protected, stabilized, and sequestered from their site of action, but under appropriate conditions, they can be readily mobilized to induce growth factor–dependent processes (i.e., neovascularization and tumor growth). Heparan sulfate molecules are also associated with the cell surface via their core protein and thus are important mediators of cell adhesion *(5).* Cleavage of heparan sulfate, therefore, results in disassembly of extracellular barriers, promoting cell invasion and releasing heparan sulfate–bound bioactive angiogenic and growth-promoting factors.

The mammalian endoglycosidase heparanase is the predominant enzyme responsible for the degradation of heparan sulfate *(7–10).* Heparanase activity may therefore play a decisive role in fundamental biologic processes associated with ECM remodeling and cell migration, such as development and morphogenesis, inflammation, angiogenesis, and cancer metastasis *(6,7,11–15).* Heparanase mRNA and protein are preferentially expressed in metastatic cell lines and human tumor tissues *(7,8,14–16).* Moreover, increased heparanase mRNA expression correlates with reduced postoperative survival of cancer patients *(17,18).* Overexpression of heparanase cDNA in tumor cells with low metastatic potential confers a high metastatic potential after the cells are injected into experimental animals *(7).* Heparanase has also been shown to elicit an angiogenic response by releasing heparan sulfate–bound angiogenic factors sequestered in the ECM *(19).* A pronounced correlation between heparanase expression and tumor microvessel density has been reported *(17,20,21).* Heparin, other sulfated polysaccharides, and heparin-mimicking molecules that inhibit heparanase enzymatic activity also reduce the incidence of metastasis in experimental animals *(12,14,22,23).* However, the use and mode of action of these compounds remains questionable because they lack specificity *(24,25).*

This study was undertaken to explore alternative strategies for heparanase inhibition by using gene-silencing technologies to specifically suppress heparanase expression *in vitro* and *in vivo* and to determine whether heparanase has a role in cancer invasion, metastasis, and angiogenesis. We used a hammerhead ribozyme approach, which is known to be highly effective in gene silencing *(26,27).* This method uses the homology of a complementary RNA to specifically target an mRNA. To generate a hammerhead ribozyme, a catalytic ribozyme core is flanked by sequences complementary to the target mRNA, which brings the catalytic region into proximity with the targeted mRNA and leads to its cleavage *(26).* The advantage of this approach over other types of antisense technology is that one ribozyme molecule can cleave many copies of the target mRNA, and thus relatively low levels of ribozyme can achieve efficient inactivation of the target gene. This method is particularly suitable for reducing the amount of abundant mRNAs *(26,27).* We have designed a hammerhead anti-heparanase ribozyme and explored whether ribozyme-mediated inhibition of heparanase expression affects invasive and adhesive properties of mouse and human cancer cells *in vitro,* as well as their metastatic and angiogenic potentials *in vivo.* We also used RNA interfering (RNAi) gene-silencing because this approach is characterized by increased stability and specificity of targeting and has potential therapeutic applications *(28,29).* We designed a highly specific anti-heparanase siRNA and constructed a vector that enabled its stable expression in cancer cells. The inhibitory effect of siRNA-mediated silencing of endogenous heparanase on mouse B16-BL6 melanoma cell invasion *in vitro* and lung colonization *in vivo* was then investigated.

Materials and Methods

Cell Lines

Methylcholanthrene-induced non-metastatic Eb (L5178Y) T lymphoma cells were provided by Dr. V. Schirrmacher (DKFZ, Heidelberg, Germany) *(30,31);* cHpaEb cells were obtained by stable transfection of Eb lymphoma cells with the chimeric form of heparanase (cHpa), composed of the human enzyme and the chicken heparanase signal sequence *(32).* Rat glioma C-6 cells were kindly provided by Dr. Eli Keshet (Hebrew University, Jerusalem, Israel). All cells were grown in RPMI-1640 supplemented with 10% fetal calf serum (FCS), L-glutamine, and antibiotics. Human breast carcinoma MDA-MB-435 and mouse B16-BL6 melanoma cells were purchased from the American Type Culture Collection (Manassas, VA). Cells were cultured in Dulbecco's Modified Eagle Medium (DMEM) containing glucose at 4.5 g/L supplemented with 10% FCS, L-glutamine, and antibiotics.

Synthesis of Anti-Heparanase Hammerhead Ribozymes

Six anti-heparanase hammerhead ribozymes (HpaRz 1–6) and a control ribozyme (ContRz) that contains the hammerhead catalytic unit but lacks specific heparanase mRNA recognition motifs were generated by *in vitro* transcription of a single-stranded oligonucleotide template encoding the T7 RNA polymerase promoter followed by a specific ribozyme coding sequence. Two micrograms of each template was transcribed by using 10 U of T7 RNA polymerase in a buffer containing 40 m*M* Tris–HCl (pH 7.5), 10 m*M* $MgCl_2$, 5 m*M* dithiothreitol, 400 μ*M* dNTP, and 50 μg/mL bovine serum albumin (BSA). The transcription reaction was performed at 37 °C for 30 minutes and was stopped by heating at 75 °C for 10 minutes. Reaction products were subjected to electrophoresis in a denaturing 15% polyacrylamide gel, visualized by ultraviolet illumination on a thin-layer chromatography screen, excised from the gel, and purified by ethanol precipitation as described *(33).*

Synthesis of Labeled Heparanase RNA Substrate for Ribozyme Cleavage

To produce the template for heparanase RNA substrate transcription, a 1487-base-pair (bp) fragment was amplified from the full-length heparanase cDNA and subcloned into the pcDNA3 plasmid (Invitrogen, Carlsbad, CA) by using polymerase chain reaction (PCR). The following two primers were used: upper primer, containing the T7 RNA polymerase promoter sequence (5′-GTAATACGACTCACTATAGGTGAGCCCCTCGTTCC TGTCCGTCACCAT-3′) and lower primer (5′-TTTTATTTT CAGATGCAGCAGC-3′). The PCR conditions included an initial denaturation at 94 °C for 2 minutes and 30 cycles of denaturation at 94 °C for 15 seconds, annealing at 55 °C for 45 seconds, and extension at 72 °C for 1 minute. Aliquots (15 μL)

of the amplified cDNA were separated by electrophoresis through a 1.5% agarose gel, and the cDNA bands were visualized by ethidium bromide staining *(7).* The 1487-bp PCR product was isolated and used as a template for the *in vitro* transcription of the heparanase RNA substrate used in the ribozyme cleavage assay. Transcription was performed with 10 U of T7 RNA polymerase in a buffer containing 40 m*M* Tris–HCl (pH 7.5), 10 m*M* $MgCl_2$, 5 m*M* dithiothreitol, 400 μ*M* [^{32}P]-labeled dNTP, and 50 μg/mL BSA at 37 °C for 30 minutes. The reaction was stopped by heat inactivation at 75 °C for 10 minutes. The substrate was subjected to electrophoresis in a denaturing 5% polyacrylamide gel and visualized after subsequent autoradiography.

In Vitro Ribozyme Cleavage Reaction

Analysis of ribozyme cleavage in a cell-free system was performed as described elsewhere *(33).* Briefly, the radioactively labeled heparanase RNA substrate, prepared as described above, was incubated with each one of the six anti-heparanase ribozymes (HpaRz 1–6) and control ribozyme (ContRz) in a molar ratio of 1:50 (ribozyme:substrate), at 37 °C for 15 and 60 minutes. Cleavage products were separated by electrophoresis in a denaturing 5% polyacrylamide gel and visualized by autoradiography.

Construction of Ribozyme Expression Vector

Vectors for the expression of the anti-heparanase ribozyme (HpaRz2) and the control ribozyme (ContRz) were constructed by subcloning DNA fragments that encode for HpaRz2 or ContRz into the expression vector pcDNA3, which contains a gene for hygromycin B resistance (Invitrogen). The oligonucleotide 5′-AGCTTGGCTTCTTCTGATGAGGCCGAAAGGCCGAAAGTAGGTGC-3′ and the complementary oligonucleotide 5′-GGCCGCACCTACTTTCGGCCTTTCGGCCTCATCAGAAGAAGCCA-3′ were used to generate the HpaRz2 ribozyme, and the oligonucleotides 5′-AGCTTGCGAAGAACTGATGAGGCCGAAAGGCCGAAACATCCAG-3′ and 5′-GATCCTGGATGTTTCGGCCTTTCGGCCTCATCAGTTCTTCGCA-3′ were used to generate the ContRz ribozyme. Each oligonucleotide was annealed to its complement by mixing equal molar amounts, heating to 80 °C, and cooling to 30 °C slowly. The double-stranded DNA was then subcloned into the multiple cloning site (at *Hin*dIII and *Not*I) of pcDNA3. For both HpaRz2 and ContRz, the sequence of the insert and the region flanking the insert was confirmed by DNA sequencing.

Construction of siRNA Expression Vectors

We used the pSUPER vector (kindly provided by Dr. R. Agami, Division of Tumor Biology, The Netherlands Cancer Institute, Amsterdam, The Netherlands) in which siRNA expression is driven by the H1 RNA promoter to produce small and size-defined RNA transcripts that lack poly-A tails. We generated two different siRNAs. The oligonucleotides 5′-GATCCCCTCTCAAGTCAACCATGATATTCAAGAGATATCATGGTTGACTTGAGATTTTTGGAAA-3′ and 5′-AGCTTTTCCAAAAATCTCAAGTCAACCATGATATCTCTTGAATATCATGGTTGACTTGAGAGGG-3′ were used to generate anti-heparanase siRNA Si1, and oligonucleotides 5′-GATCCCCACTCCAGGTGGAATGGCCCTTCAAGAGAGGGCCATTCCACCTGGAGTTTTTTGGAAA-3′ and 5′-AGCTTTTCCAAAAAACTCCAGGTGGAATGGCCCTCTCTTGAAGGGCCATTCCACCTGGAGTGGG-3′ were used to generate anti-heparanase siRNA Si2. Each oligonucleotide pair (100 pmol) was annealed by incubation at 95 °C for 5 minutes and cooled slowly. One microliter of this mixture was then ligated into the pSUPER vector *(34),* which had been digested with *Bgl*II and *Hin*dIII. As a result, two vectors, pSi1 and pSi2, expressing Si1 and Si2 siRNA were generated. The empty pSUPER vector was used as a control.

Transfection

Eb lymphoma (0.5×10^6 cells per milliliter) or MDA-MB-435 breast carcinoma (0.3×10^6 cells per milliliter) cells were incubated (48–72 hours at 37 °C) with a total of 1–2 μg of DNA and 6 μL of FuGene transfection reagent (Boehringer, Mannheim, Germany) in 94 μL of Optimem (Gibco-BRL, Gaithersburg, MD) *(35,36).* Transfected Eb cells were selected with 200 μg/mL hygromycin B (Sigma) and 350 μg/mL G418 (Gibco-BRL). Transfected MDA-MB-435 cells were selected with 200 μg/mL hygromycin B. Stable transfected cells were obtained and routinely maintained in selection medium to avoid overgrowth of non-transfected cells. B16-BL6 melanoma cells were electroporated with pSi1, pSi2, or empty pSUPER constructs (4×10^6 cells in 400 μL of medium containing 10 μg of plasmid DNA) by using a single 70-ms pulse at 140 V and an ECM 830 Electro Square porator and disposable cuvettes (model 640, 4-mm gap; BTX, San Diego, CA). After electroporation, the transfected cells were plated at a density of 0.4×10^6 cells per 100-mm dish and allowed to grow for 24–48 hours. Efficiency of transfection (≈80%) was evaluated 48 hours after electroporation of a vector containing the gene encoding green fluorescent protein by fluorescence microscopy.

RNA Isolation and Reverse Transcription–PCR

RNA was isolated from 5×10^6 tumor cells with TRIzol (Invitrogen), according to the manufacturer's instructions, and quantified by spectrophotometry. After oligo(dT)-primed reverse transcription of 500 ng of total RNA, the resulting single-stranded cDNA was amplified using TaqDNA polymerase and buffer (Promega, Madison, WI). The primers used were HPU-355 (5′-TTCGATCCCAAGAAGGAATCAAC-3′) and HPL-229 (5′-GTAGTGATGCCATGTAACTGAATC-3′) for human heparanase; 431-U (5′-ATGCTCTACAGTTTTGCCAAGTG-3′) and 876-L (5′-CAGAATTTTTTGCACAGAGAGAA-3′) for mouse heparanase; glyceraldehyde 3-phosphate dehydrogenase (GAPDH) S (5′-CCACCCATGGCAAAATTCCATGGCA-3′) and GAPDH-AS (5′-TCTAGACGGCAGGTCAGGTCCACC-3′) for human GAPDH; L-19-U (5′-ATGCCAACTCTCGTCAACAG-3′) and L-19-L (5′-GCGCTTTCGTGCTTCCTT-3′) for mouse L19; and HygR-U (5′-AGACCTGCCTGAAACCGAAC-3′) and HygR-L (5′-CCGCTCGTCTGGCTAAGAT-3′) for the hygromycin B resistance (hygromycin phosphotransferase) gene expressed by both pHpaRz2 and pContRz vectors. PCR conditions for the expression of human genes included an initial denaturation of 4 minutes at 94 °C followed by 26 cycles of denaturation for 45 seconds at 94 °C, annealing for 1 minute at 60 °C, and extension for 1 minute at 72 °C. PCR conditions for the expression of mouse genes included an initial denaturation of 2 minutes at 95 °C followed by 24 cycles of denaturation for 15 seconds at 96 °C, annealing for 70 seconds

at 58 °C, and extension for 80 seconds at 72 °C (24 cycles). Aliquots (10 μL) of the amplification products were separated by electrophoresis through a 1.5% agarose gel and visualized by ethidium bromide staining. The intensity of each band was quantified using Scion Image software (Scion, Frederick, MD). Only RNA samples that gave completely negative results in PCR without reverse transcriptase were used to rule out the presence of genomic DNA contamination.

Heparanase Activity

Tumor cell lysates prepared from 1×10^6 cells by three cycles of freezing and thawing in reaction buffer (20 m*M* phosphate–citrate buffer containing 1 m*M* dithiothreitol, 1 m*M* $CaCl_2$, and 50 m*M* NaCl) were incubated (5 hours, 37 °C [pH 6.6]) with ^{35}S-labeled ECM, prepared as described *(37).* The incubation medium was centrifuged (20 000*g*, 4 °C, 15 minutes), and the supernatant containing ^{35}S-labeled heparan sulfate degradation fragments was analyzed by gel filtration on a Sepharose CL-6B column (0.9 × 30 cm). Fractions (0.2 mL) were eluted with phosphate-buffered saline (PBS), and the amount of radioactivity in each fraction was counted in a beta scintillation counter *(7,12,30).* Each experiment was performed at least three times, and the variation in elution positions (K_{av} values) did not exceed 15%. Reaction buffer with or without recombinant human heparanase (1 ng/mL) was routinely used as a positive or negative control, respectively.

Immunohistochemistry

MDA-MB-435 cells transfected with pHpaRz2 or pContRz were seeded on round glass coverslips in 4-well plates. After 24 hours, the cells were washed twice with PBS and fixed with chilled (–20 °C) 100% methanol for 3 minutes. The cells were then washed five times with PBS, and the intrinsic fluorescence was blocked by treating the cells with 50 m*M* NH_4Cl for 5 minutes at room temperature. The cells were then washed three times with PBS, incubated in PBS with 5% goat serum and 0.1% Triton X-100 for 30 minutes at room temperature (24 °C), and washed twice with PBS. Slides were incubated for 2 hours at 24 °C with polyclonal anti-heparanase antibodies (10 μg/mL pAb 733 in PBS with 5% goat serum) *(38),* washed five times with PBS, and incubated with Cy-3-conjugated goat anti-rabbit immunoglobulin G (1:100 diluted in PBS; Jackson, Bar Harbor, ME) for 1 hour at 24 °C. Slides were then washed eight times with PBS, mounted with 90% glycerol in PBS, and examined microscopically with a Zeiss LSM 410 confocal microscope *(32,36).*

Tissue sections for immunostaining were obtained from formalin-fixed and paraffin-embedded primary tumors produced in mice by subcutaneously injected cHpaEb lymphoma cells transfected with pHpaRz2 or pContRz vectors. Immunostaining was performed with anti-human heparanase monoclonal antibody (mAb 130, kindly provided by InSight Biopharmaceuticals, Rehovot, Israel) and horseradish peroxidase–conjugated goat anti-mouse antibodies (Histostatin-*PLUS* Bulk Kit; Zymed Laboratories, San Francisco, CA), as described *(7).* Vascular endothelial cells in tumor tissue sections were stained with anti-Von Willebrand polyclonal antibodies (Dako, Golstrup, Denmark) as described *(39).* Negative controls without addition of primary antibody showed low background staining in all cases.

Proliferation Assay

MDA-MB-435 breast carcinoma cells (5×10^5 cells per 100-mm dish) and cHpaEb lymphoma cells (2×10^5 cells per 75-mL flask) that were stably transfected with pHpaRz2 or control vectors and B16-BL6 melanoma cells (3×10^5 cells per 100-mm dish) that were transiently transfected with anti-heparanase pSi2 or control vectors were seeded in complete media in triplicate. The cells were harvested and counted in triplicate with a Coulter counter (Coulter Electronics, Luton, U.K.) every other day for 7 days, as described *(22).* The breast carcinoma and melanoma cells were dissociated into single-cell suspensions with trypsin and EDTA before counting.

Matrigel Invasion Assay

Tumor cells (3×10^5 cells in 1 mL of DMEM containing 0.1% BSA) were assayed in triplicate for Matrigel invasion at 37 °C in a humidified incubator (95% air, 5% CO_2) for 6 hours, by using Boyden blind-well chemotaxis chambers (NeuroProbe, Gaithersburg, MD) and polycarbonate filters (13 mm in diameter, 8-μm pore size; Costar Scientific, Cambridge, MA) coated with Matrigel, as described *(40,41).* Medium conditioned by NIH3T3 fibroblasts was used as a chemoattractant and placed in the lower compartment of the Boyden chamber *(40).* For a negative control, serum-free DMEM containing 0.1% BSA was placed in the lower compartment of the Boyden chamber instead of the chemoattractant. After 6 hours, the filters were removed and the cells on the lower surface of the filter were stained with reagents from the Diff-Quik kit (American Scientific Products, McGaw Park, IL). The total number of cells from five microscopic fields selected at random (×100 magnification) was counted for each well.

Invasiveness of the Eb lymphoma cells was determined by using a modified invasion assay. Because staining Eb cells with the reagents from the Diff-Quik kit is not effective, the cells were first labeled with [^{3}H]thymidine (1×10^6 cells, 48 hours, 37 °C, 1 μCi/mL [^{3}H]thymidine, Amersham, Buckinghamshire, U.K.). Cell invasion was performed as described above and quantified by counting triplicate Matrigel-coated filters in a beta scintillation counter *(35).* Before the radioactivity was counted, cells from the upper side of the filter were removed with a cotton swab. Each experiment was repeated three times.

Cell Adhesion

Eb cells were grown (1×10^6 cells per milliliter, 48 hours, 37 °C) in RPMI-1640 medium supplemented with 10% FCS (complete medium) in the presence of [^{3}H]thymidine (1 μCi/mL). The labeled cells were washed three times in complete medium to remove unincorporated thymidine, added to ECM-coated wells (1×10^6 cells per well in four-well plates) in triplicate, and incubated at 37 °C in complete medium (pH 7.2) for 15 minutes *(35).* In some experiments, adhesion of transfected cHpaEb cells to dishes coated with a naturally produced ECM, prepared as described in *(37),* was tested. After the incubation, the wells were washed three times with serum-free medium and the remaining firmly adhered cells were lysed in 0.2 *M* NaOH for 2 hours at 37 °C. The lysates were counted in a beta scintillation counter. Each experiment was repeated three times.

Experimental and Spontaneous Metastasis

For the experimental metastasis studies, the lateral tail vein of 6-week-old male C57BL/6 mice was injected with 0.4 mL of a cell suspension containing 0.4×10^6 B16-BL6 melanoma cells transiently transfected with anti-heparanase siRNA-expressing vector (pSi2) or empty pSUPER vector *(34).* Fifteen days after cell injection, mice were killed and their lungs were removed, fixed in Bouin's solution, and scored under a dissecting microscope for the number of metastatic nodules on the lung surface *(12).* Five mice were used per group, and three independent experiments were performed.

For the spontaneous metastasis studies, 2-month-old male CD1 nude mice (10 mice per group) were injected subcutaneously in the lower back with 1×10^6 Eb lymphoma cells expressing the secreted chimeric heparanase protein (cHpaEb) *(36)* or Eb lymphoma cells stably transfected with either anti-heparanase ribozyme (pHpaRz2) or control ribozyme (pContRz) expression plasmids. Five mice from each group were killed on day 11 (at this time point, live mice from the control group were still available) and examined for primary tumor size, vascularity, and liver metastasis *(36).* Metastatic colonization of the liver was evaluated by gross examination, wet weight measurements, and microscopic inspection of tissue sections. The remaining five mice from each group were monitored for survival. All animal experiments were approved by the Animal Care Committee of the Hebrew University, Jerusalem, Israel.

Statistical Analysis

InStat statistical software, version 3.05 (GraphPad Software, San Diego, CA), was used to calculate statistical differences between groups (tested by the unpaired Student's *t* test). All *P* values were two-sided.

Results

Selection of Active Anti-Heparanase Hammerhead Ribozymes

We produced six different hammerhead ribozymes (HpaRz 1–6) by *in vitro* transcription using double-stranded DNA oligonucleotides containing the T7 promoter, the conserved catalytic domain, and two flanking sequences designed to recognize specific motifs along the human heparanase mRNA, as shown for HpaRz2 (Fig. 1, A). To associate with and cleave its specific target, the hammerhead ribozyme must fold into a typical three-dimensional structure, with the folded catalytic core domain connected to the flanking complementary sequences, as shown for HpaRz2 in Fig. 1, B.

To test the effectiveness of the ribozymes, we generated a truncated heparanase RNA substrate of 1487 nucleotides that contains the recognition sites for all six anti-heparanase ribozymes (data not shown). Although the substrate showed no specific pattern of cleavage after incubation without ribozymes, distinct cleavage fragments were easily detected after incubation with each of the six ribozymes (HpaRz 1–6) individually (data not shown). HpaRz2 was the most effective ribozyme to cleave the substrate in a time-dependent manner, evidenced by almost complete degradation of the substrate and presence of the cleavage products of expected size (Fig. 1, C). It was therefore selected for use in further studies.

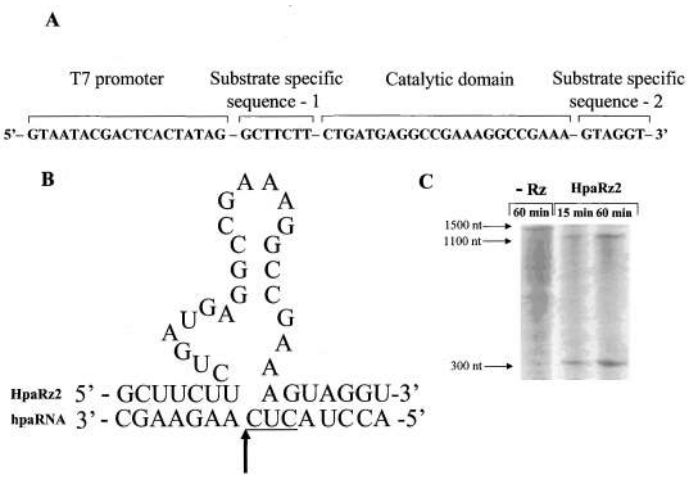

Fig. 1. Structure and *in vitro* activity of anti-heparanase hammerhead ribozyme. **A**) DNA template (sense strand) of anti-heparanase ribozyme (HpaRz2) containing a T7 promoter, two complementary substrate-specific sequences, and an invariable catalytic consensus domain. **B**) Schematic representation of HpaRz2. After *in vitro* transcription, the catalytic core forms the typical hammerhead structure as a result of the base-pair formation between complementary nucleotides. The flanking substrate-specific sequences bind the heparanase RNA substrate. **Arrow** = predicted cleavage site. **C**) *In vitro* cleavage assay using anti-heparanase ribozyme HpaRz2. The radioactively labeled heparanase RNA substrate was incubated without (- Rz) or with HpaRz2 for 15 and 60 minutes. The full-length substrate (1487 nucleotides) and cleavage products were separated and visualized by autoradiography.

Inhibition of Heparanase Activity, Cell Invasion, and Adhesion *In Vitro* Associated With Stable Expression of Anti-Heparanase Ribozyme

We constructed a vector to constitutively express the anti-heparanase ribozyme HpaRz2 (pHpaRz2) and tested its ability to inhibit the synthesis of endogenous heparanase. We stably transfected MDA-MB-435 breast carcinoma cells, which are known to express high levels of heparanase *(7),* with the pHpaRz2 vector and assayed the transfected cells for heparanase mRNA expression and enzymatic activity (Fig. 2, A). To control for possible effects of the hammerhead unit itself, MDA-MB-435 cells were transfected with the pContRz vector, which encodes for a ribozyme with an identical catalytic core but that lacks the specific heparanase mRNA recognition motifs (Fig. 2, A). Compared with MDA-MB-435 cells stably transfected with pContRz, MDA-MB-435 cells stably transfected with pHpaRz2 displayed a marked decrease in heparanase mRNA levels when evaluated by reverse transcription–PCR (RT-PCR) (Fig. 2, A, inset) and densitometric analysis (data not shown) and showed no heparanase enzymatic activity (Fig. 2, A). In addition, immunofluorescent staining with anti-heparanase antibodies revealed that MDA-MB-435 cells stably transfected with pHpaRz2 had a marked decrease in heparanase protein levels compared with MDA-MB-435 cells stably transfected with pContRz (Fig. 2, B). There was no difference in the rate of proliferation *in vitro* between cells transfected with pHpaRz2 and cells transfected with pContRz (data not shown).

Because heparanase plays a role in cell invasion through the ECM and basement membrane *(7,13,36),* we tested the effect of anti-heparanase ribozyme on MDA-MB-435 invasive ability. MDA-MB-435 cells stably transfected with pHpaRz2 or pContRz were compared for their ability to invade a reconstituted base-

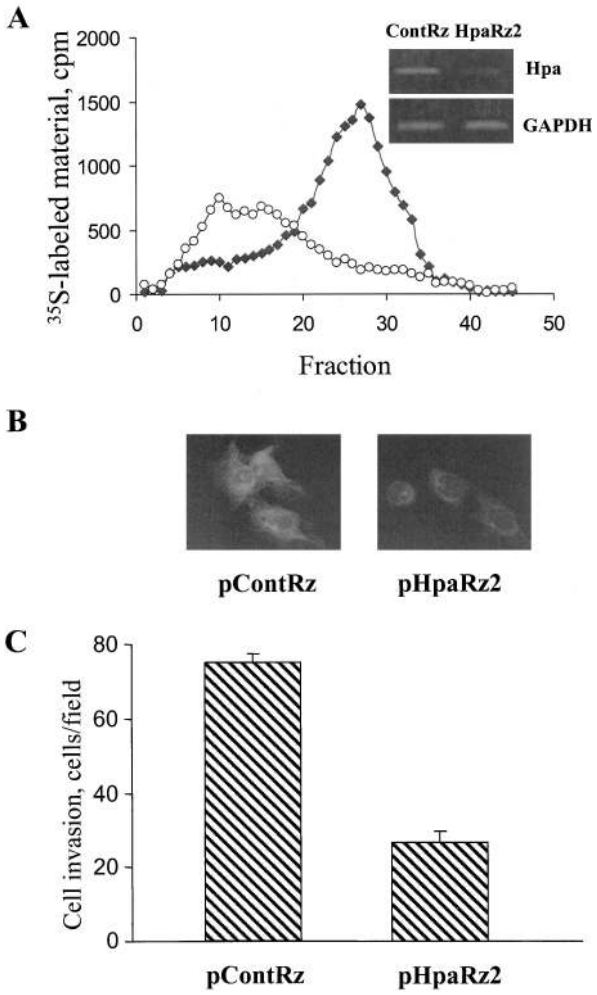

Fig. 2. Effect of anti-heparanase hammerhead ribozyme HpaRz2 on endogenous heparanase expression, enzymatic activity, and invasiveness of MDA-MB-435 cells. **A**) Heparanase mRNA levels in MDA-MB-435 cells stably transfected with the plasmid pHpaRz2 or the control plasmid pContRz were assessed by semiquantitative reverse transcription–polymerase chain reaction (RT-PCR). RT-PCR products obtained with glyceraldehyde 3-phosphate dehydrogenase (GAPDH) primers were used as a control for RNA integrity and equal loading (**inset**). To measure heparanase activity, lysates from MDA-MB-435 cells stably transfected with pHpaRz2 (○) or pContRz (♦) were incubated with ^{35}S-labeled extracellular matrix *(37),* and the ^{35}S-labeled degradation fragments released into the incubation medium were analyzed by gel filtration *(8,12,30).* **B**) Immunofluorescent staining of heparanase expressed in MDA-MB-435 cells stably transfected with pHpaRz2 (**right**) or pContRz (**left**). Heparanase was detected with a rabbit anti-heparanase polyclonal antibody *(38)* and a Cy-3-conjugated secondary antibody. **C**) *In vitro* invasiveness through Matrigel *(40,41)* was measured in MDA-MB-435 cells stably transfected with pHpaRz2 or with pContRz. The mean number of cells per field on the lower surface of the filter was determined from five random microscopic fields per filter and from three filters per cell type. The experiment was repeated three times. **Error bars** show upper 95% confidence intervals.

ment membrane (Matrigel) *(41).* Compared with MDA-MB-435 cells stably transfected with pContRz (mean number of cells per field = 75.2, 95% CI = 72.8 to 77.6), the invasive ability of MDA-MB-435 cells stably transfected with pHpaRz2 (mean number of cells per field = 26.8, 95% CI = 24.2 to 29.4) statistically significantly decreased by 64% ($P<.001$) (Fig. 2, C). Similar results were obtained with C-6 rat glioma cells, which had been genetically engineered to express high levels of human heparanase (data not shown).

Next, we used Eb lymphoma cells, which lack endogenous heparanase activity *(30).* Eb lymphoma cells were engineered to express a readily secreted chimeric form of heparanase (cHpa), composed of the human enzyme and the chicken heparanase signal sequence *(32).* We previously demonstrated that Eb cells expressing cHpa (cHpaEb) degraded heparan sulfate in ECM to a much greater extent than non-transfected Eb cells or cells transfected with the non-secreted human enzyme *(32).* Moreover, cHpaEb cells had increased invasiveness and metastatic potential in mice *(36)* and are therefore a useful experimental model for the study of heparanase involvement in tumor progression. In this study, cHpaEb cells stably transfected with pHpaRz2 or pContRz were tested for heparanase activity (Fig. 3, A) and their ability to invade Matrigel *in vitro* (Fig. 3, B). Compared with cHpaEb cells stably transfected with pContRz, cHpaEb cells stably transfected with pHpaRz2 had a marked decrease of more than 70% in heparanase-mediated degradation of heparan sulfate, demonstrating that the secreted form of heparanase was efficiently targeted by the ribozyme. Compared with cHpaEb cells stably transfected with pContRz, the amount of radioactivity associated with cHpaEb cells stably transfected with pHpaRz2 that invaded the Matrigel was statistically significantly reduced by 54% from 112.2×10^3 cpm (95% CI = 108.6×10^3 to 115.8×10^3 cpm) to 50.9×10^3 cpm (95% CI = 49.1×10^3 to 52.7×10^3 cpm; $P<.001$) (Fig. 3, B). There was no difference in the rate of proliferation *in vitro* between cHpaEb cells transfected with pHpaRz2 and cHpaEb cells transfected with pContRz (data not shown).

Recently, heparanase has been shown to promote cell adhesion to ECM, independently of its enzymatic properties *(35).* To test whether expression of the heparanase ribozyme affected heparanase-mediated cell adhesion, we compared the adhesive ability of cHpaEb cells stably transfected with pHpaRz2 with that of cHpaEb cells stably transfected with pContRz. As shown in Fig. 3, C, expression of the heparanase ribozyme effectively inhibited adhesion of transfected cHpaEb cells to dishes coated with a naturally produced ECM. By contrast, there was no difference in the adhesive ability of untreated cHpaEb cells and those treated with laminaran sulfate, a potent inhibitor of heparanase enzymatic activity *(22)* (data not shown).

Effect of Anti-Heparanase Ribozyme on Lymphoma Primary Tumor Vascularization, Metastasis, and Mortality of Tumor-Bearing Mice

We next investigated the effect of ribozyme-mediated heparanase gene silencing on the metastatic potential of cHpaEb lymphoma cells stably transfected with either pHpaRz2 or pContRz injected subcutaneously into nude mice. The mice were monitored for survival time and liver metastases. All mice injected with cells transfected with pHpaRz2 survived during the first 3 weeks of the experiment (Fig. 4, A). By contrast, all mice injected with cells transfected with pContRz, the control inactive ribozyme, were dead by day 14 (Fig. 4, A). On day 11, livers of five randomly selected mice from each group were removed, weighed, and processed for histological examination (Fig. 4, B). Gross macroscopic examination of the livers revealed numerous lymphoma metastases in all of the mice injected with pContRz-transfected cells but few or no visible metastatic nodules in the livers of mice injected with pHpaRz2-transfected cells (Fig. 4, B, top). The liver weights of mice injected with pContRz-

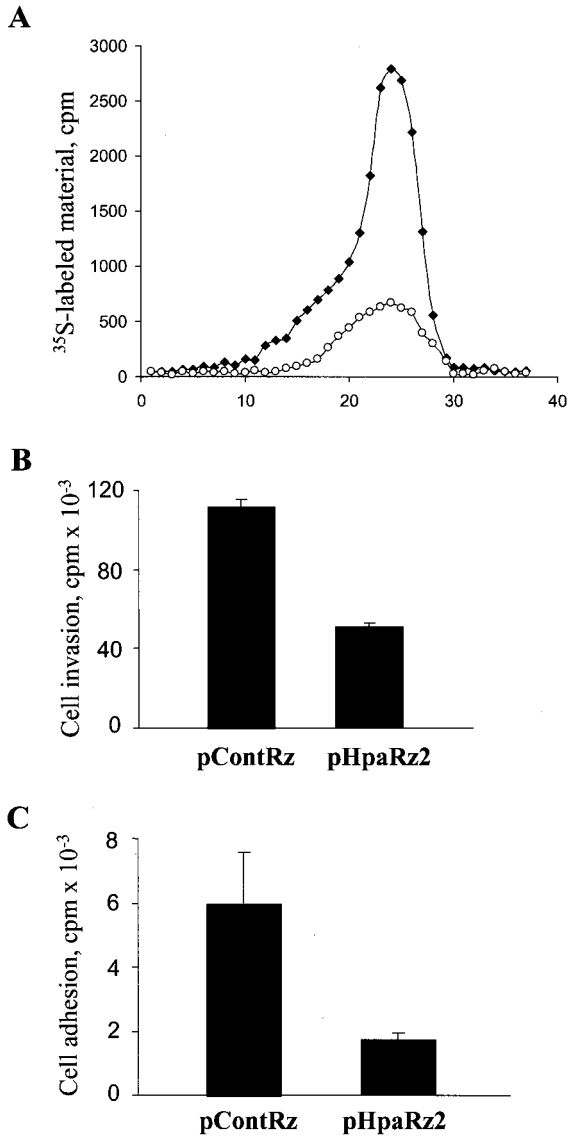

Fig. 3. Effect of anti-heparanase hammerhead ribozyme HpaRz2 on heparanase activity and lymphoma cell invasion and adhesion. **A**) Heparanase activity in lysates from Eb lymphoma cells expressing a chimeric heparanase (cHpaEb) and transfected with the plasmid pHpaRz2 (o) or the control plasmid pContRz (♦) was determined by incubating lysates with ^{35}S-labeled extracellular matrix *(37).* The ^{35}S-labeled degradation fragments released into the incubation medium were analyzed by gel filtration *(8,12,30).* **B**) *In vitro* invasiveness through Matrigel was measured using [^{3}H]thymidine-labeled cHpaEb cells transfected with pHpaRz2 or pContRz. The cells were incubated (1×10^{6} cells per milliliter) on top of Matrigel-coated filters, and the extent of cell invasion was measured by counting the filters in a beta scintillation counter. The experiment was repeated three times. The data represent the mean of three independent experiments with 95% confidence intervals. **C**) Cell adhesion to extracellular matrix (ECM) was measured using [^{3}H]thymidine-labeled cHpaEb cells transfected with pHpaRz2 or pContRz. Cells were suspended in RPMI medium, seeded on unlabeled ECM *(37),* and allowed to attach for 15 minutes at 37 °C. After extensively washing the cells to remove unincorporated [^{3}H]thymidine and unattached cells, the attached cells were lysed, and the amount of radioactivity was counted in a beta scintillation counter. Data are the means of three independent experiments, and **error bars** show upper 95% confidence intervals.

transfected cHpaEb cells (mean weight = 4.7 g, 95% CI = 4.5 to 5.9 g) were statistically significantly higher than the liver weights of mice injected with pHpaRz2-transfected cHpaEb cells (mean weight = 2.0 g, 95% CI = 1.9 to 2.1 g; $P<.001$) (Fig. 4, B, middle). In fact, the liver weight of mice injected with pHpaRz2-transfected cHpaEb cells was similar to that of control mice (mean weight = 1.7 g, 95% CI = 1.5 to 1.7 g). Microscopic examination of liver tissue sections revealed a massive infiltration of the liver by pContRz-transfected cells but little or no liver infiltration by pHpaRz2-transfected cells (Fig. 4, B, bottom).

In addition, subcutaneous primary tumors formed by pHpaRz2- or pContRz-transfected cHpaEb cells were examined for vascularity. A marked decrease in blood content and hemorrhage was noted by gross examination of tumors produced by cHpaEb cells stably transfected with pHpaRz2 relative to tumors produced by cells transfected with pContRz (Fig. 4, C, top). Whereas tumors produced by cells transfected with pContRz were dark-reddish, tumors produced by cells transfected with pHpaRz2 appeared pale (Fig. 4, C, top). The decreased vascularity of tumors produced by pHpaRz2 (i.e., active) versus pContRz (i.e., control) ribozyme-transfected cells was confirmed by histologic examination of the respective tissue sections stained with anti-Von Willebrand Factor antibody (Fig. 4, C, middle). Counting the blood vessels revealed a statistically significant ($P<.001$) difference in the vascular density of tumors produced by pHpaRz2-transfected cHpaEb cells (mean number of vessels = 15.3, 95% CI = 10.4 to 20.2) compared with tumors produced by pContRz-transfected cells (mean number of vessels = 40.8, 95% CI = 34.6 to 46.9) (Fig. 4, C, bottom).

To ensure that expression of the HpaRz2 and control ribozymes from the pHpaRz2 and pContRz vectors in the lymphoma cells was preserved throughout the *in vivo* experiment, total RNA was extracted from subcutaneous tumors produced by pHpaRz2- and pContRz-transfected cHpaEb cells. The tumors were excised 2 weeks after cell injection, and the presence of the hygromycin-resistance gene mRNA, equally expressed by both vectors, was demonstrated by RT-PCR (data not shown). Immunostaining of the tumor tissue with a monoclonal antibody (mAb 130) directed against human heparanase revealed intense staining of lymphoma cells in sections derived from tumors produced by cells transfected with pContRz but very weak or no staining in tumors produced by cells transfected with pHpaRz2 (Fig. 4, D). This result clearly demonstrates that heparanase gene silencing in pHpaRz2-transfected cHpaEb cells persisted throughout the duration of the *in vivo* experiment.

siRNA-Mediated Heparanase Silencing and Invasive and Metastatic Potential of B16-BL6 Melanoma Cells

To further elucidate the direct involvement of heparanase in tumor progression and the effectiveness of endogenous heparanase gene silencing, we applied the siRNA targeting approach, using highly metastatic B16-BL6 mouse melanoma cells, which contain high levels of endogenous heparanase *(12,22).* Two siRNA variants (Si1 and Si2) targeting two different regions of the mouse heparanase mRNA were designed and cloned into the pSUPER plasmid *(34)* to generate pSi1 and pSi2 expression vectors.

B16-BL6 mouse melanoma cells were transiently transfected with pSi1, pSi2, or empty pSUPER (mock) vectors by electroporation, and the cells were tested for heparanase expression and activity 48 hours later. Cells transfected with pSi1 or pSi2 contained 70%–80% less heparanase mRNA than mock-

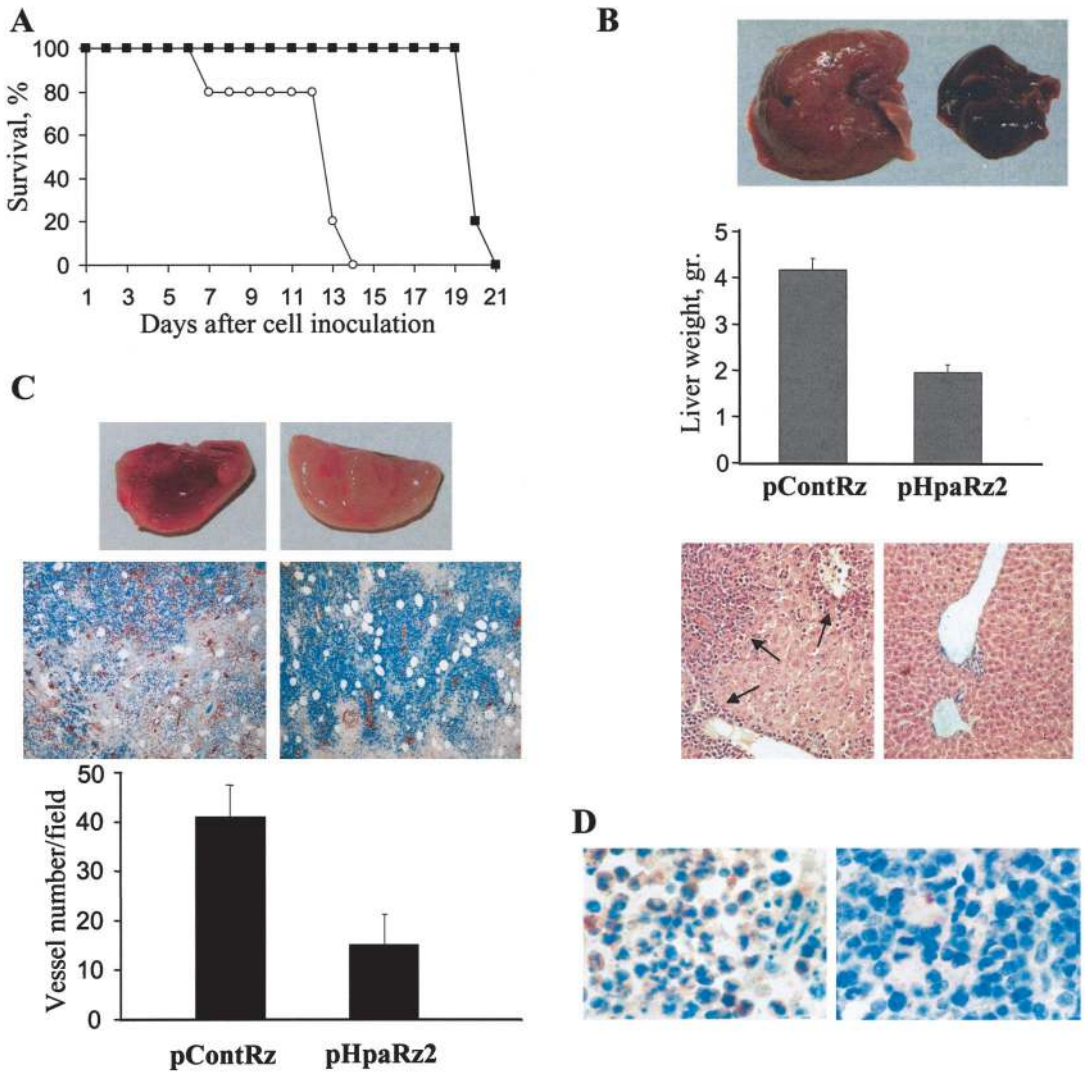

Fig. 4. Effect of anti-heparanase hammerhead ribozyme HpaRz2 on mortality, liver metastasis, and tumor angiogenesis *in vivo.* **A**) The survival of CD1 nude mice inoculated subcutaneously with 1 × 10^6 Eb lymphoma cells expressing chimeric heparanase (cHpaEb) and transfected with the plasmid pHpaRz2 (■) or pContRz (○) (n = 10 mice per group). Mice were monitored daily for survival time. **B**) On day 11 of the experiment, five mice from each group were killed and their livers were dissected, weighed, and examined. **Top panel** = livers from mice injected with pHpaRz2-transfected (**right**) and pContRz-transfected (**left**) lymphoma cells. **Middle panel** = mean weight with upper 95% confidence interval. **Bottom panel** = histologic analysis of hematoxylin and eosin–stained sections of liver tissue from mice injected with pHpaRz2-transfected (**right**) and pContRz-transfected (**left**) lymphoma cells. Original magnification = ×200. **Arrows** mark liver colonization by pContRz-transfected cHpaEb cells. **C**) On day 11, tumors produced by cHpaEb cells transfected with pHpaRz2 or pContRz were excised, photographed, processed for histology, and examined for tumor vascularity. **Top panel** = gross appearance. Tumors produced by cHpaEb cells transfected with pContRz (**left**) appeared dark-reddish, whereas tumors produced by cHpaEb cells transfected with pHpaRz2 (**right**) appeared pale, reflecting a marked difference in vascularity, blood content, and hemorrhage. **Middle** and **bottom panels** = microvessel density in the primary tumor tissue was quantified in formalin-fixed sections (5 μm thick) of tumors produced by cHpaEb cells transfected with pContRz (**left**) or pHpaRz2 (**right**) after being stained with an anti-Von Willebrand Factor antibody (reddish staining). Original magnification = ×200 (**middle panel**). Vascular density (vessels per microscopic field) was determined by counting five randomly selected fields per tumor and four tumors per group. **Bars** represent the means of vessel count. **Error bars** show 95% confidence intervals (**bottom panel**). **D**) Heparanase immunostaining of cHpaEb tumors *in vivo.* Paraffin-embedded tissue sections of primary tumors produced by cHpaEb lymphoma cells transfected with pContRz (**left**) or pHpaRz2 (**right**) vectors were stained with monoclonal anti-heparanase antibody (reddish staining). Original magnification = ×400. Note the extensive staining in tumors produced by pContRz-transfected cells versus weak or no staining in tumors formed by pHpaRz2-transfected cells.

transfected cells, as determined by semiquantitative RT-PCR (Fig. 5, A). Heparanase enzymatic activity, measured in cell lysates, was markedly lower (60% and 75%, respectively) in lysates from pSi1- and pSi2-transfected cells than in lysates from mock-transfected cells, further demonstrating effective silencing of the heparanase gene by heparanase-targeted siRNA (Fig. 5, B). The duration of siRNA-mediated heparanase silencing was determined by measuring heparanase enzymatic activity in B16-BL6 cells at various time points after electroporation with the anti-heparanase pSi2 vector. Maximal effect of siRNA silencing was observed 48 hours after electroporation, and it declined thereafter. The difference in levels of heparanase activity between mock-transfected cells and siRNA-transfected cells was less pronounced by 72 hours and even more so by 96 hours (nearly a 50% decrease in heparanase enzymatic activity in siRNA- versus mock-transfected cells). By 8–9 days after transfection, there was no detectable difference in heparanase activity between siRNA- and mock-transfected cells (data not shown).

In subsequent experiments, we tested the effect of heparanase-targeted siRNA on B16-BL6 cell invasiveness using the Matrigel invasion assay. The ability of B16-BL6 cells to invade through Matrigel-coated filters was statistically significantly ($P<.001$) inhibited 48 hours after transfection with pSi1 (mean number of cells per field = 57.4, 95% CI = 48.2 to 66.6) or pSi2 (mean number of cells per field = 40.6, 95% CI = 35.6 to 45.6) compared with cells transfected with vector alone (mean number of cells per field = 121.4, 95% CI = 118.9 to 123.9) (Fig. 5, C).

Finally, we tested the effect of siRNA-mediated heparanase silencing on experimental metastasis *in vivo.* For this purpose, B16-BL6 cells were electroporated with pSi2 or the empty vector. After 48 hours, when silencing of the heparanase gene had reached its maximum, the cells were injected

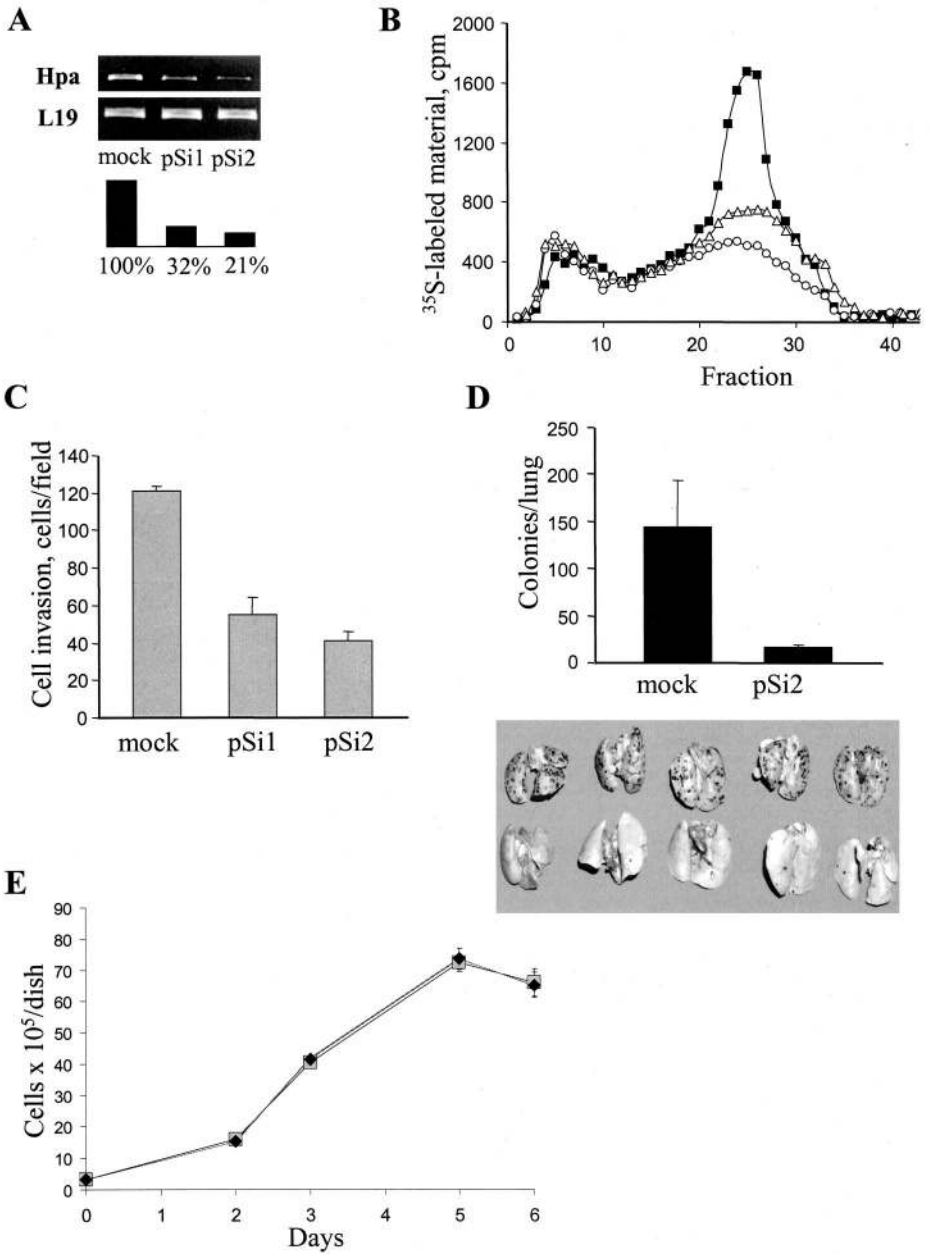

Fig. 5. RNA interference and B16-BL6 mouse melanoma cell heparanase enzymatic activity, Matrigel invasion, and lung colonization. **A**) **Top:** Heparanase mRNA levels in murine B16-BL6 melanoma cells transfected with the anti-heparanase small interfering RNA (siRNA) expression vectors pSi1, pSi2, or empty control pSUPER vector (mock), were assessed by semiquantitative reverse transcription–polymerase chain reaction (RT-PCR) with primers specific for mouse heparanase (**upper panel**). RT-PCR products obtained with L19-specific primers were used as a control for RNA integrity and equal loading (**lower panel**). **Bottom:** The intensity of each band was quantified using the Scion Image program, and the results are expressed as a percentage of band intensity relative to that of L19. **B**) Heparanase activity in B16-BL6 melanoma cells transfected with the anti-heparanase siRNA pSi1 (△), pSi2 (○), or empty (■) vectors was assessed after 48 hours. Lysates were incubated with ^{35}S-labeled extracellular matrix, and the ^{35}S-labeled degradation fragments released into the incubation medium were analyzed by gel filtration *(8,12,30).* **C**) *In vitro* cell invasion through Matrigel was assessed in B16-BL6 melanoma cells 48 hours after transfection with pSi1, pSi2, or with vector alone. The mean number of cells per field on the lower surface of the filter was determined from five random microscopic fields per filter and from three filters per cell type. The experiment was repeated three times. **Error bars** show 95% confidence intervals. **D**) *In vivo* lung colonization of B16-BL6 melanoma cells transfected with either mock or pSi2 vectors and injected intravenously into C57BL/6 mice. After 15 days, mice were killed, and their lungs were fixed and examined for the number of melanoma colonies on the lung surface. **Top:** Bars represent the mean number of colonies per lung from five mice. **Error bars** show upper 95% confidence interval. **Bottom:** Gross appearance of lungs of mice injected with mock-transfected (**upper panel**) or siRNA-transfected (**lower panel**) B16-BL6 melanoma cells. **E**) Proliferation was measured in B16-BL6 melanoma cells electroporated with anti-heparanase siRNA pSi2 (♦) or empty (□) vectors. Cells were seeded in 100-mm dishes at an initial density of 3×10^5 cells per dish. Cells were dissociated and counted in triplicate every other day for 6 days. Each point represents mean ± 95% confidence intervals of triplicate wells.

into the tail vein of C57BL/6 mice (0.4×10^6 cells per mouse). In this experimental metastasis model, the invasive properties of the tumor cells are critical for their extravasation, primarily during the first 3 hours after the tumor cells enter into the circulation *(12,42–44).* Therefore, the transient, noncontinuous silencing of heparanase in B16-BL6 cells allows for the identification of parameters directly involved in blood-borne tumor dissemination, such as the contribution of heparanase to cell extravasation as opposed to its possible effects on subsequent survival of the melanoma colonies in the target organ, stromal support, and secondary metastasis. Fifteen days after injection, the mice were killed, and their lungs were evaluated for the number of surface metastatic colonies. B16-BL6 melanoma cells transiently transfected with pSi2 established statistically significantly fewer metastatic colonies (mean number of colonies = 16.0, 95% CI = 13.4 to 18.6) than B16-BL6 melanoma cells transiently transfected with the empty vector (mean number of colonies = 144.3, 95% CI = 95.1 to 193.5; $P<.001$) (Fig. 5, D).

To ensure that the observed *in vitro* and *in vivo* effects were not a result of differences in the proliferative ability of B16-BL6 melanoma cells transfected with the pSi2 and control vectors, we compared the rate of proliferation of the two cell types. Mock- and pSi2-transfected B16-BL6 cells had the same rate of proliferation *in vitro* (Fig. 5, E). Thus, these data clearly demonstrate that specific silencing of endogenous heparanase gene expres-

sion effectively inhibits the invasive and metastatic potential of B16-BL6 melanoma cells.

Discussion

Numerous data suggest that heparanase plays an important role in sustaining the pathology of malignant tumors. Expression of heparanase is associated with the aggressiveness of tumor cell lines *(7,8,13–15,45).* Increased levels of the enzyme were detected in the sera of animals bearing metastatic tumors, in the sera of patients with cancer, and in the urine of some patients with aggressive metastatic disease *(2,14),* reflecting an association between abnormal heparanase secretion and metastatic disease. Moreover, the heparanase gene and protein are overexpressed in human cancers, including those of the bladder *(17),* colon *(16),* stomach *(46),* breast *(47),* oral cavity *(48),* esophagus *(49),* pancreas *(18,50,51),* and brain *(52),* and in multiple myeloma *(21)* and acute myeloid leukemia *(53).* These results and the unexpected occurrence of a single functional heparanase enzyme *(12–15),* indicate that the heparanase enzyme may be an attractive target for the development of an anticancer therapy.

Various polyanionic compounds capable of inhibiting heparanase enzymatic activity, such as heparin, laminaran sulfate *(22),* and maltohexaose sulfate *(23),* have antitumor and antimetastatic activities. However, because of the multiple biologic activities of these compounds *(24,25),* the mechanism of their antitumor activity and its relation to heparanase inhibition are not straightforward. Moreover, the pleiotropic interactions of these compounds with the ECM and the cell surface might produce nonspecific and undesirable effects *(24,25).* Similarly, studies on the involvement of heparanase in cancer progression are hampered by the lack of effective neutralizing anti-heparanase antibodies. Recently, an attempt to use a more specific antisense approach has been reported *(54),* although in that animal model, the tumor cells were injected intrathoracically, which is not typical for metastasis studies. Hence, cells injected intrathoracically are not required to undergo intravasation or extravasation and do not encounter extracellular barriers to invade, such as the subendothelial basement membrane. In addition, among the currently available gene-silencing methods, the antisense approach is regarded as being of limited value because of its known sequence-independent effects and limited efficacy *(55).*

In this study, we used two powerful gene-silencing strategies (ribozyme and siRNA) to functionally inactivate the heparanase gene in diverse cellular and animal tumor models. Ribozyme targeting led to a marked inhibition of *in vitro* invasive and adhesive potentials of cells that either naturally express increased levels of the endogenous enzyme (i.e., MDA-MB-435 human breast carcinoma) *(7)* or were genetically engineered to overexpress the human heparanase gene (C-6 glioma, Eb lymphoma) *(36).* The anti-heparanase ribozyme statistically significantly inhibited the spontaneous metastases of cHpaEb cells to the liver. This effect was reflected in increased survival of mice injected with cHpaEb lymphoma cells expressing the anti-heparanase ribozyme relative to that of mice injected with cells expressing a control ribozyme. Moreover, vascularization of cHpaEb primary tumors was also markedly suppressed in cells that were transfected with the anti-heparanase ribozyme. The observed anti-angiogenic effect of the anti-heparanase ribozyme is primarily the result of an indirect effect of heparanase silencing on the bioavailability of angiogenesis-promoting factors that are sequestered by heparan sulfate in the tumor microenvironment and can be released by the tumor-derived heparanase *(13,19).*

The biologic and therapeutic relevance of the heparanase-silencing approach was further validated using the highly metastatic B16-BL6 mouse melanoma cells *(12)* transfected with mouse heparanase-specific siRNA. Knockdown of heparanase expression resulted in an almost complete inhibition (≈80%) of lung colonization after intravenous injection of siRNA-transfected B16-BL6 cells compared with mock-transfected cells. Previous studies *(12,42–44)* clearly established that in the B16-BL6 experimental metastasis model, invasive properties of the tumor cells are critical for cell extravasation, primarily during the first few hours after the tumor cells enter into the bloodstream. Based on the kinetics of heparanase siRNA silencing in transiently transfected B16-BL6 melanoma cells cultured *in vitro,* the *in vivo* experiments were designed to have maximal heparanase silencing occur during the first several hours after cells were injected into the bloodstream. Transient, noncontinuous silencing of heparanase in B16-BL6 cells restricted the suppression of heparanase activity to the critical window of blood-borne cell extravasation, followed by release of the inhibitory effect during the subsequent formation of metastatic colonies in the lungs. Thus, we have specifically analyzed the role of heparanase in cell extravasation rather than in the multiple subsequent events, such as cell proliferation and establishment and survival of colonies in the target organ and angiogenesis and formation of secondary metastases.

To our knowledge, the data described here represent the first successful application of ribozyme- and siRNA-mediated gene silencing to effectively reduce the levels of heparanase. Our results highlight a critical role of heparanase in tumor angiogenesis, growth, and metastasis. In addition to demonstrating the potential promise for cancer treatment, the specific heparanase gene-silencing tools clarify the molecular and cellular mechanisms underlying recently described heparanase-mediated processes such as cell adhesion *(35,56)* and survival signals *(56,57) in vitro,* as well as tissue repair, hair growth *(39),* and bone formation *in vivo* (Zcharia E, Kram V, Yacobi-Zeevi Y, Bab I, Vlodavsky I: unpublished data). These tools, which target RNA, are especially important in light of the recently discovered nonenzymatic functions of heparanase *(35,56)*—functions that are not sensitive to the currently available heparanase inhibitors *(22,23).* For example, we found that heparanase-mediated cell adhesion was markedly inhibited in HpaRz-transfected lymphoma cells but not by laminaran sulfate, which efficiently inhibits heparanase enzymatic activity *(12,22).* Heparanase gene silencing may thus provide novel mechanistic insights into the functions of heparanase (i.e., cell adhesion and signal transduction) unobtainable by other methods of inhibiting heparanase enzymatic activity.

Further investigation is required to identify the most effective delivery strategies for therapy using ribozyme and siRNA gene-silencing approaches. Experiments are underway to test the feasibility of electroporating heparanase-targeted siRNA-expressing vectors directly into the primary tumor *in vivo (58).* Of particular promise is the development of lentivirus-based vectors that enable sustained expression of heparanase-silencing agents in the target tumor cells *(59).* Such a vector has already

been constructed and will be administered systemically or locally by electroporation into the tumor tissue. The ability of a lentivirus to infect both dividing and nondividing cells and to allow for long-term multilineage gene expression *(60)* will extend the range of cells and tumor types in which the heparanase-silencing approach may be practical.

REFERENCES

(1) Liotta LA, Kohn EC. The microenvironment of the tumour-host interface. Nature 2001;411:375–9.

(2) Vlodavsky I. Involvement of the extracellular matrix, heparan sulphate proteoglycans, and heparan sulphate degrading enzymes in angiogenesis and metastasis. In: Bicknell R, Lewis CE, Ferrara N, editors. Tumour angiogenesis. Oxford (U.K.): Oxford University Press; 1997. p. 125–40.

(3) Kalluri R. Basement membranes: structure, assembly and role in tumour angiogenesis. Nat Rev Cancer 2003;3:422–33.

(4) Timpl R. Macromolecular organization of basement membranes. Curr Opin Cell Biol 1996;8:618–24.

(5) Bernfield M, Gotte M, Park PW, Reizes O, Fitzgerald ML, Lincecum J, et al. Functions of cell surface heparan sulfate proteoglycans. Annu Rev Biochem 1999;68:729–77.

(6) Vlodavsky I, Bar-Shavit R, Ishai-Michaeli R, Bashkin P, Fuks Z. Extracellular sequestration and release of fibroblast growth factor: a regulatory mechanism? Trends Biochem Sci 1991;16:268–71.

(7) Vlodavsky I, Friedmann Y, Elkin M, Aingorn H, Atzmon R, Ishai-Michaeli R, et al. Mammalian heparanase: gene cloning, expression and function in tumor progression and metastasis. Nat Med 1999;5:793–802.

(8) Hulett MD, Freeman C, Hamdorf BJ, Baker RT, Harris MJ, Parish CR. Cloning of mammalian heparanase, an important enzyme in tumor invasion and metastasis. Nat Med 1999;5:803–9.

(9) Kussie PH, Hulmes JD, Ludwig DL, Patel S, Navarro EC, Seddon AP, et al. Cloning and functional expression of a human heparanase gene. Biochem Biophys Res Commun 1999;261:183–7.

(10) Toyoshima M, Nakajima M. Human heparanase. Purification, characterization, cloning, and expression. J Biol Chem 1999;274:24153–60.

(11) Vlodavsky I, Eldor A, Haimovitz-Friedman A, Matzner Y, Ishai-Michaeli R, Lider O, et al. Expression of heparanase by platelets and circulating cells of the immune system: possible involvement in diapedesis and extravasation. Invasion Metastasis 1992;12:112–27.

(12) Vlodavsky I, Mohsen M, Lider O, Svahn CM, Ekre HP, Vigoda M, et al. Inhibition of tumor metastasis by heparanase inhibiting species of heparin. Invasion Metastasis 1994;14:290–302.

(13) Vlodavsky I, Friedmann Y. Molecular properties and involvement of heparanase in cancer metastasis and angiogenesis. J Clin Invest 2001;108:341–7.

(14) Nakajima M, Irimura T, Nicolson GL. Heparanases and tumor metastasis. J Cell Biochem 1988;36:157–67.

(15) Parish CR, Freeman C, Hulett MD. Heparanase: a key enzyme involved in cell invasion. Biochim Biophys Acta 2001;1471:M99–108.

(16) Friedmann Y, Vlodavsky I, Aingorn H, Aviv A, Peretz T, Pecker I, et al. Expression of heparanase in normal, dysplastic, and neoplastic human colonic mucosa and stroma. Evidence for its role in colonic tumorigenesis. Am J Pathol 2000;157:1167–75.

(17) Gohji K, Okamoto M, Kitazawa S, Toyoshima M, Dong J, Katsuoka Y, et al. Heparanase protein and gene expression in bladder cancer. J Urol 2001;166:1286–90.

(18) Koliopanos A, Friess H, Kleeff J, Shi X, Liao Q, Pecker I, et al. Heparanase expression in primary and metastatic pancreatic cancer. Cancer Res 2001;61:4655–9.

(19) Elkin M, Ilan N, Ishai-Michaeli R, Friedmann Y, Papo O, Pecker I, et al. Heparanase as mediator of angiogenesis: mode of action. FASEB J 2001;15:1661–3.

(20) Watanabe M, Aoki Y, Kase H, Tanaka K. Heparanase expression and angiogenesis in endometrial cancer. Gynecol Obstet Invest 2003;56:77–82.

(21) Kelly T, Miao HQ, Yang Y, Navarro E, Kussie P, Huang Y, et al. High heparanase activity in multiple myeloma is associated with elevated microvessel density. Cancer Res 2003;63:8749–56.

(22) Miao HQ, Elkin M, Aingorn E, Ishai-Michaeli R, Stein CA, Vlodavsky I. Inhibition of heparanase activity and tumor metastasis by laminarin sulfate and synthetic phosphorothioate oligodeoxynucleotides. Int J Cancer 1999;83:424–31.

(23) Parish CR, Freeman C, Brown KJ, Francis DJ, Cowden WB. Identification of sulfated oligosaccharide-based inhibitors of tumor growth and metastasis using novel in vitro assays for angiogenesis and heparanase activity. Cancer Res 1999;59:3433–41.

(24) Borsig L, Wong R, Feramisco J, Nadeau DR, Varki NM, Varki A. Heparin and cancer revisited: mechanistic connections involving platelets, P-selectin, carcinoma mucins, and tumor metastasis. Proc Natl Acad Sci U S A 2001;98:3352–7.

(25) Koenig A, Norgard-Sumnicht K, Linhardt R, Varki A. Differential interactions of heparin and heparan sulfate glycosaminoglycans with the selectins. Implications for the use of unfractionated and low molecular weight heparins as therapeutic agents. J Clin Invest 1998;101:877–89.

(26) Sigurdsson ST, Eckstein F. Structure-function relationships of hammerhead ribozymes: from understanding to applications. Trends Biotechnol 1995;13:286–9.

(27) Kashani-Sabet M, Funato T, Florenes VA, Fodstad O, Scanlon KJ. Suppression of the neoplastic phenotype in vivo by an anti-ras ribozyme. Cancer Res 1994;54:900–2.

(28) Sharp PA. RNA interference–2001. Genes Dev 2001;15:485–90.

(29) Elbashir SM, Harborth J, Lendeckel W, Yalcin A, Weber K, Tuschl T. Duplexes of 21-nucleotide RNAs mediate RNA interference in cultured mammalian cells. Nature 2001;411:494–8.

(30) Vlodavsky I, Fuks Z, Bar-Ner M, Ariav Y, Schirrmacher V. Lymphoma cell-mediated degradation of sulfated proteoglycans in the subendothelial extracellular matrix: relationship to tumor cell metastasis. Cancer Res 1983;43:2704–11.

(31) Larizza L, Schirrmacher V, Pfluger E. Acquisition of high metastatic capacity after in vitro fusion of a nonmetastatic tumor line with a bone marrow-derived macrophage. J Exp Med 1984;160:1579–84.

(32) Goldshmidt O, Zcharia E, Aingorn H, Guatta-Rangini Z, Atzmon R, Michal I, et al. Expression pattern and secretion of human and chicken heparanase are determined by their signal peptide sequence. J Biol Chem 2001;276:29178–87.

(33) Hubinger G, Schmid M, Linortner S, Manegold A, Bergmann L, Maurer U. Ribozyme-mediated cleavage of wt1 transcripts suppresses growth of leukemia cells. Exp Hematol 2001;29:1226–35.

(34) Brummelkamp TR, Bernards R, Agami R. A system for stable expression of short interfering RNAs in mammalian cells. Science 2002;296:550–3.

(35) Goldshmidt O, Zcharia E, Cohen M, Aingorn H, Cohen I, Nadav L, et al. Heparanase mediates cell adhesion independent of its enzymatic activity. FASEB J 2003;17:1015–25.

(36) Goldshmidt O, Zcharia E, Abramovitch R, Metzger S, Aingorn H, Friedmann Y, et al. Cell surface expression and secretion of heparanase markedly promote tumor angiogenesis and metastasis. Proc Natl Acad Sci U S A 2002;99:10031–6.

(37) Vlodavsky I. Preparation of extracellular matrices produced by cultured corneal endothelial and PF-HR9 endodermal cells. In: Bonifacino JS, Dasso M, Harford JB, Lippincott-Schartz J, Yamada KM, editors. Current protocols in cell biology. New York (NY): John Wiley & Sons; 1999;Suppl 1:10.4.1–4.14.

(38) Zetser A, Levy-Adam F, Kaplan V, Gingis-Velitsky S, Bashenko Y, Schubert S, et al. Processing and activation of latent heparanase occurs in lysosomes. J Cell Sci 2004;117:2249–58.

(39) Zcharia E, Metzger S, Chajek-Shaul T, Aingorn H, Elkin M, Friedmann Y, et al. Transgenic expression of mammalian heparanase uncovers physiological functions of heparan sulfate in tissue morphogenesis, vascularization and feeding behavior. FASEB J 2004;18:252–63.

(40) Elkin M, Reich R, Nagler A, Aingorn E, Pines M, de-Groot N, et al. Inhibition of matrix metalloproteinase-2 expression and bladder carcinoma metastasis by halofuginone. Clin Cancer Res 1999;5:1982–8.

(41) Albini A, Iwamoto Y, Kleinman HK, Martin GR, Aaronson SA, Kozlowski JM, et al. A rapid in vitro assay for quantitating the invasive potential of tumor cells. Cancer Res 1987;47:3239–45.

(42) Fidler IJ. Metastasis: quantitative analysis of distribution and fate of tumor embolilabeled with 125 I-5-iodo-2′-deoxyuridine. J Natl Cancer Inst 1970;45:773–82.

(43) Fidler IJ. Biological behavior of malignant melanoma cells correlated to their survival in vivo. Cancer Res 1975;35:218–24.
(44) Esumi N, Fan D, Fidler IJ. Inhibition of murine melanoma experimental metastasis by recombinant desulfatohirudin, a highly specific thrombin inhibitor. Cancer Res 1991;51:4549–56.
(45) Nakajima M, Irimura T, Di Ferrante D, Di Ferrante N, Nicolson GL. Heparan sulfate degradation: relation to tumor invasive and metastatic properties of mouse B16 melanoma sublines. Science 1983;220:611–3.
(46) Tang W, Nakamura Y, Tsujimoto M, Sato M, Wang X, Kurozumi K, et al. Heparanase: a key enzyme in invasion and metastasis of gastric carcinoma. Mod Pathol 2002;15:593–8.
(47) Maxhimer JB, Quiros RM, Stewart R, Dowlatshahi K, Gattuso P, Fan M, et al. Heparanase-1 expression is associated with the metastatic potential of breast cancer. Surgery 2002;132:326–33.
(48) Ikuta M, Podyma KA, Maruyama K, Enomoto S, Yanagishita M. Expression of heparanase in oral cancer cell lines and oral cancer tissues. Oral Oncol 2001;37:177–84.
(49) Mikami S, Ohashi K, Usui Y, Nemoto T, Katsube K, Yanagishita M, et al. Loss of syndecan-1 and increased expression of heparanase in invasive esophageal carcinomas. Jpn J Cancer Res 2001;92:1062–73.
(50) Kim AW, Xu X, Hollinger EF, Gattuso P, Godellas CV, Prinz RA. Human heparanase-1 gene expression in pancreatic adenocarcinoma. J Gastrointest Surg 2002;6:167–72.
(51) Rohloff J, Zinke J, Schoppmeyer K, Tannapfel A, Witzigmann H, Mossner J, et al. Heparanase expression is a prognostic indicator for postoperative survival in pancreatic adenocarcinoma. Br J Cancer 2002;86:1270–5.
(52) Marchetti D, Nicolson GL. Human heparanase: a molecular determinant of brain metastasis. Adv Enzyme Regul 2001;41:343–59.
(53) Bitan M, Polliack A, Zecchina G, Nagler A, Friedmann Y, Nadav L, et al. Heparanase expression in human leukemias is restricted to AML. Exp Hematol 2002;30:34–41.
(54) Uno F, Fujiwara T, Takata Y, Ohtani S, Katsuda K, Takaoka M, et al. Antisense-mediated suppression of human heparanase gene expression inhibits pleural dissemination of human cancer cells. Cancer Res 2001;61:7855–60.
(55) Van Oekelen D, Luyten WH, Leysen JE. Ten years of antisense inhibition of brain G-protein-coupled receptor function. Brain Res Brain Res Rev 2003;42:123–42.
(56) Zetser A, Bashenko Y, Miao HQ, Vlodavsky I, Ilan N. Heparanase affects adhesive and tumorigenic potential of human glioma cells. Cancer Res 2003;63:7733–41.
(57) Gingis-Velitski S, Zetser A, Flugelman MY, Vlodavsky I, Ilan N. Heparanase induces endothelial cell migration via protein kinase B/Akt activation. J Biol Chem 2004;279:23536–41.
(58) Tamura T, Sakata T. Application of in vivo electroporation to cancer gene therapy. Curr Gene Ther 2003;3:59–64.
(59) Matta H, Hozayev B, Tomar R, Chugh P, Chaudhary PM. Use of lentiviral vectors for delivery of small interfering RNA. Cancer Biol Ther 2003;2:206–10.
(60) Rubinson DA, Dillon CP, Kwiatkowski AV, Sievers C, Yang L, Kopinja J, et al. A lentivirus-based system to functionally silence genes in primary mammalian cells, stem cells and transgenic mice by RNA interference. Nat Genet 2003;33:401–6.

NOTES

Supported by grant 532/02 from the Israel Science Foundation; by Public Health Service grant R01-CA106456-01 from the National Cancer Institute, National Institutes of Health, Department of Health and Human Services; and by funding from the Susan G. Komen Breast Cancer Foundation, the Center for the Study of Emerging Diseases (CSED), and the European Commission (5th Framework program, contract QLKCT-2002-02049).

We thank Dr. Yaron Tikochinski (Intelegene) and Dr. Helena Aingorn (Department of Oncology, Hadassah-University Hospital) for their excellent advice and continuous support.

Manuscript received January 25, 2004; revised June 3, 2004; accepted June 16, 2004.